Growth and optical characterization of indirect-gap $Al_xGa_{1-x}As$ alloys

E. Purón, G. Martínez-Criado,[a)] and I. Riech
Facultad de Física-IMRE, Universidad de La Habana, 10400-Vedado, C. Habana, Cuba

J. Almeida-García
Institut de Physique Appliquée, École Polytechnique Fédérale, 1015-Lausanne, Switzerland

A. Cantarero
Departamento de Física Aplicada, Universidad de Valencia, 46100-Burjasot, Valencia, Spain

Nonintentionally doped $Al_xGa_{1-x}As$ layers with $0.38 \leq x \leq 0.84$ were grown on (100) GaAs substrates by liquid phase epitaxy (LPE) under near-equilibrium conditions. The crystalline quality of the samples was studied by photoluminescence at 2 K and room temperature Raman spectroscopy. The peculiar behavior in the photoluminescence intensities of the indirect bound exciton line and the donor–acceptor pair transition is explained from the evolution of the silicon donor binding energy according to the aluminum composition. It was also possible to observe the excitonic transition corresponding to the $Al_xGa_{1-x}As$/GaAs interface, despite the disorder and other factors which are normally involved when growing high-aluminum-content layers by this technique. Furthermore, Raman measurements show the quadratic variations of longitudinal optical phonon frequencies with aluminum concentration in good agreement with previous experimental results. In this work we show that high quality indirect-gap $Al_xGa_{1-x}As$ samples can be grown by LPE under near-equilibrium conditions. © *1999 American Institute of Physics.* [S0021-8979(99)00413-2]

PACS 78.55, 78.66.B, 81.15.L

I. INTRODUCTION

Liquid phase epitaxy (LPE), compared with molecular beam epitaxy (MBE) or metalorganic chemical vapor deposition (MOCVD), still continues being a useful technique for obtaining optoelectronic devices based on III–V compounds.[1–6] The quality and properties of the grown layers depend to a great extent on the initial state of the growth solution; for this reason, it is recommended to use supercooling alloys in the first step of the growth procedure.[7,8] Obtaining layers from saturated solutions (near-equilibrium conditions) requires a high accuracy throughout all the steps followed in the process.[8,9] A recent study reports that the defects (gallium antisites) found by growing with a certain supercooling cannot be appreciated in photoluminescence (PL) measurements even though the formation of terraces can be morphologically present growing from saturation solutions.[10]

Among the large quantity of III–V materials obtained by LPE, the $Al_xGa_{1-x}As$/GaAs system has occupied a privileged position for more than 20 years. Therefore, its optical and electrical properties have been extensively studied.[11–15] However, only a few papers have reported on the experimental behavior of both bound exciton (BE) recombination and free-electron–acceptor ($e^- - A°$) transition in the indirect gap range.[16–18] In contrast to what happens for the direct bound exciton, the coincidence between these results is poor. In a significant part, this is due to the fact that factors such as disorder, internal stresses, crystalline defects and impurities become relevant.[19,20]

In addition, some disagreements have been shown between the compositional dependencies of the longitudinal optical (LO) vibrational modes obtained by Raman spectroscopy. For instance, a recent paper shows a lineal dependence for the $LO(\Gamma)$ GaAs-like mode,[21] in contrast to the traditional quadratic relations.[15,22,23] Certainly, these differences are relatively small but not less important if keeping in mind that these relationships are commonly used to calibrate the aluminum content.

For these reasons, this paper presents low temperature (LT) photoluminescence and room temperature (RT) Raman spectroscopy data of the indirect band gap $Al_xGa_{1-x}As$ alloy. The samples were grown on (100) GaAs substrates by LPE under near-equilibrium conditions. From PL measurements it can be reaffirmed that high crystalline and interfacial quality epitaxial layers are obtained when growing from saturated solutions. Furthermore, the variation of the LO modes with the aluminum composition is studied over the complete aluminum mole fraction range.

II. EXPERIMENTAL DETAILS

Liquid-phase epitaxial layers of $Al_xGa_{1-x}As$ were grown on (100) Sn-doped GaAs substrates ($n = 1.6 \times 10^{18}$ cm^{-3}) in a conventional horizontal system. During the baking time the melt was maintained in a flux of high-purity H_2 atmosphere by means of a Pd cell. Ga and Al elements (4N and 5N purities, respectively) and high-purity polycrystalline GaAs (residual impurities concentration $\leq 10^{13}$ cm^{-3}) were used to saturate the solution. In spite of

[a)]Present address: Departamento de Física Aplicada, Universidad de Valencia, Spain; Electronic mail: gmc@uv.es

the low purity of the elemental sources with respect to to-day's standards, an average background Hall carrier concentration of about 7×10^{15} cm^{-3} was achieved by a long-term prebaking of the solutions. This result is of the same order of magnitude as those already reported in high quality AlGaAs films $(1-5 \times 10^{15}$ cm$^{-3})$.[7,24] All the samples were grown under the same conditions, i.e., initial temperature $T = 755 °C$, cooling rate $R = 1 °C/min$, and a growth time of 20 min. The weights of the materials used to prepare the growth solutions were calculated from the solubility curves for the AlGaAs ternary system[25] for an equilibrium temperature of 755 °C. The thicknesses of the epitaxial layers were obtained from the cleaved cross sections.

Photoluminescence spectra at 2 and 10 K were measured with a conventional system. As exciting sources the 488 and 514.5 nm Ar$^+$ lines were impinged on the sample contained in a close-helium cryostat. Typical laser power densities used for recording the spectra were 40 mW/cm^2. The luminescence emitted from the sample was focused on the entrance slit of a Spex double monochromator, model 1403, and at the exit slit the signal was detected by a Hamamatsu R636 GaAs:Cs photomultiplier tube. Synchronous detection techniques were used for signal measurements, which were implemented by using a lock-in amplifier interface with a PC computer for data processing.

For the Raman measurements, we used an XY-800 DILOR double spectrometer with a GaAs photomultiplier and photon counting techniques. The monochromator steps were 0.1 and 0.2 cm^{-1}, and the integration time of the detector ranged from 10 to 15 s. The entrance and exit slits varied from 100 to 150 μm, and the middle slit was always twice that of the entrance slit. The excitation source was a LEXEL 95-3 argon laser. The power on the sample was typically 50 mW with a spot diameter between 50 and 100 μm.

Double crystal x-ray diffractometry (DCD) measurements were carried out in a BEDE scientific instrument x-ray diffractometer to determine the aluminum content in the epilayers. The rotation step of the monochromator axis was $0.67''$, while the sample rotation step was $0.42''$. From the K_α (Cu) line (400) Bragg diffraction rocking curves, the aluminum content was obtained by measuring the angle difference $\Delta\theta$ between the GaAs and Al$_x$Ga$_{1-x}$As peaks, and using the relation $\Delta\theta = 367'' x$.[26] The average DCD rocking curve full width at half maximum (FWHM) of the Al$_x$Ga$_{1-x}$As layers was $30''$. The angular accuracy in the experiment was $2''$ which guarantees an error below 0.5% in the aluminum content determination.

III. RESULTS AND DISCUSSION

A. Photoluminescence

In the compositional range studied, the photoexcited electrons thermalize in the X minima of the conduction band, while the excited holes do it in the Γ valence band maximum. The presence of alloy disorder relaxes the k-conservation selection rule, and makes zero phonon indirect transitions possible. The behavior of the 2 K PL spectra as a function of the aluminum content is shown in Fig. 1. In general, the following transitions are of great significance: (i)
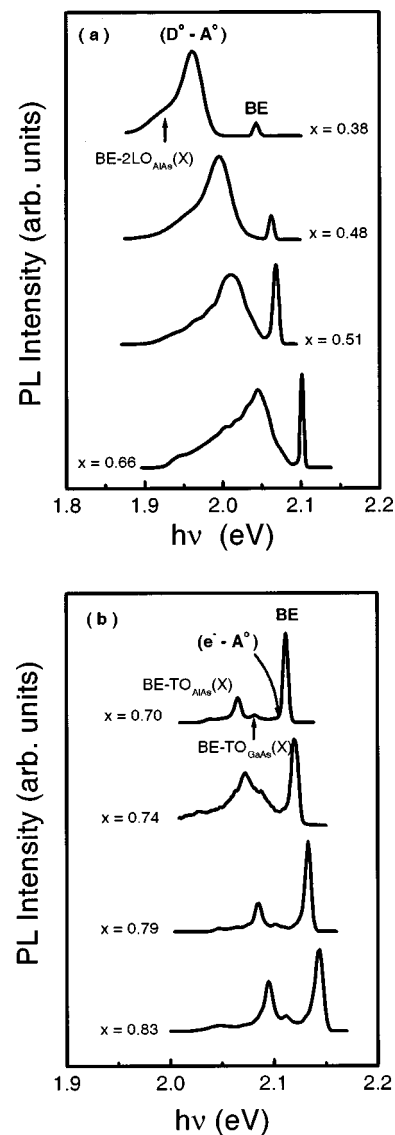

FIG. 1. Photoluminescence spectra at 2 K of nonintentionally doped Al$_x$Ga$_{1-x}$As layers with different values of Al content ($0.38 \leq x \leq 0.84$). The emission peaks are attributed to bound exciton (BE), donor–acceptor pair transitions ($D°-A°$), and BE phonon replicas (BE-2LO(X)-GaAs, BE$-$TO(X)-GaAs and BE$-$TO(X)-AlAs).

at higher energy, the emission corresponding to the indirect BE, followed by the recombinations associated with the shallow impurities: free-electron–neutral-acceptor transition $(e^--A°)$, and donor–acceptor pair recombination $(D°-A°)$, and (ii) at lower energies, the BE phonon replicas: BE-2LO(X)-GaAs, BE$-$TO(X)-GaAs and BE$-$TO(X)-AlAs. In our case, the typical residual impurities are carbon and silicon, whose origins are in the graphite crucible and the quartz reactor, respectively. In principle, both impurities are amphoteric, that is, they are donors on an element III site and acceptors on an element V site. However, up to now carbon has been found only as an acceptor in Al$_x$Ga$_{1-x}$As.[15]

The expected BE shift towards larger energies is seen as the aluminum content increases. Furthermore, for $0.38 \leq x \leq 0.66$, the BE/$(D°-A°)$ intensity ratio increases [Fig. 1 (a)] and simultaneously, the energy distance between both emis-
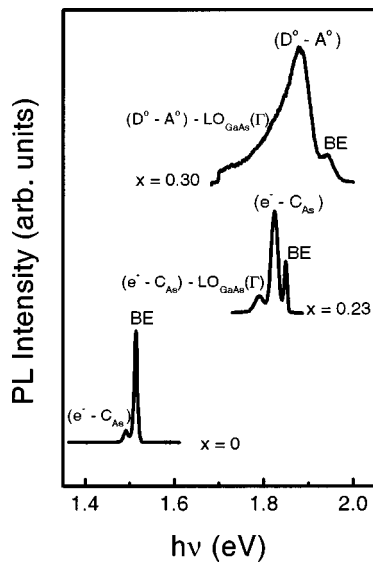
FIG. 2. Photoluminescence spectra at 2 K of three direct gap $Al_xGa_{1-x}As$ layers with different values of Al content ($x=0$, 0.23 and 0.30). The emission peaks are attributed to bound exciton (BE), free electron–neutral-acceptor transition ($e^--A^°$), donor–acceptor pair transition ($D^°-A^°$), and phonon replicas of ($e^--A^°$) and ($D^°-A^°$) recombinations.

TABLE I. Energy position of the four ($D^°-A^°$) bands for Si doped $Al_xGa_{1-x}As$ in the $0.38 \leq x \leq 0.84$ compositional range.[a]

Transition	$h\nu$ (eV)
$(D_1^°-A^°)$	$1.493 + 1.28x$
$(D_2^°-A^°)$	$2.009 - 0.43x + 0.91x^2$
$(D_3^°-A^°)$	$1.583 + 1.14x - 0.63x^2$
$(D_4^°-A^°)$	$1.570 + 0.75x$

cal dependence of the carbon donor ionization energy has been found for x values up to 0.4:[29]

$$BE(x) = 26.7 + 5.6x + 110x^{3.4}, \qquad (1)$$

whereas in Ref.18 experimental data have been reported for the indirect band gap range. In the latter case, the ionization energy increases from 41.7 meV for $x=0.48$ up to 64.9 meV for $x=0.90$, similar to our results (Table II). On the other hand, the silicon donor ionization energy obtained from the temperature dependence of the Hall carrier concentration is lower than 10 meV for $x<0.2$, and about 60 meV for layers with $x>0.5$.[30] In the crossover region this ionization energy notably rises, having a maximum for $x=0.45$, in accordance with our impurity binding energy behavior mentioned before.

Thus, only the dependence of the ($D^°-A^°$) pair transition with the aluminum content remains to be analyzed. The silicon has four kinds of donor levels associated in the crossover region:[31] a donor D_1, associated with the Γ valley, a donor D_4, associated with the L valley and two donors, D_2 and D_3, associated with the L and X valleys, respectively. These donors give rise to four donor to acceptor emission bands. Table I shows the x dependence of the donor–acceptor emissions at low temperature and in the $0.18 \leq x \leq 0.63$ compositional range.[15,31]

Therefore, at the crossover the L minima, the emissions bands are almost resonant with the other two minima; and for these x values the occupation density of the L valley is large and the donor that regulates the free carrier concentration is the deep level associated with the L valley. For this reason, the apparent binding energy of the silicon donor increases in the crossover region, as has been reported by Hall measurements.[30] At the same time, we can observe a single wide ($D^°-A^°$) band which results from the overlapping of the ($D_2^°-A^°$), ($D_3^°-A^°$) and ($D_4^°-A^°$) bands due to the spread of the donor–acceptor pair distance and the decrease of the D_1 donor binding energy. The prevalence of a donor over the others and the appearance of a particular ($D^°-A^°$) transition is also determined by different factors such as sample quality, disorder impurity profile and defects. On the other hand, the broadening observed and the reduction of the bound exciton intensity could also be due to the compositional disorder and the intervalley scattering present in the alloy concentration range studied here.[15]

With the aim of analyzing all the transitions in more detail, a standard multi-Gaussian fitting procedure was applied to each spectrum of Fig. 1. In Table II, the results concerning the fundamental transitions as well as the layer thickness are shown. In general, the layer thickness decreases

sions decreases. Instead, for $0.66 \leq x \leq 0.84$ the behavior is significantly different: the ($D^°-A^°$) pair emission is not observed, dominating the phonon replicas of the bound exciton peak: $BE-TO(X)$-GaAs and $BE-TO(X)$-AlAs [Fig. 1(b)]. This evolution can be understood if we compare the PL spectra observed in direct gap AlGaAs samples with different aluminum content (Fig. 2).

From Figs. 1 and 2 we can conclude that when the aluminum concentration goes towards the crossover ($x_{cr} = 0.38$) approaching from both the left side ($x<x_{cr}$) and the right side ($x>x_{cr}$), the corresponding impurity transitions intensify and become broader to join with the closest emissions. Simultaneously, the impurity binding energies increase and these emissions move away from the excitonic line, which loses intensity as they approach to the crossover region.

It is important to note that the abrupt transformation of the spectra as the alloy composition changes from 0.66 to 0.70 is likely associated with the behavior of the aluminum content in the melt. Layers with high Al composition are obtained from solutions with high quantities of aluminum and small fractions of arsenic. Therefore, it is possible that the combined effect of this factor, the very high reactivity of the molten Al, and the temperature dependence of the Al segregation coefficient, reduces the impurity incorporation.[27,28] As a consequence, the ($D^°-A^°$) pair recombination intensity decreases, making this transition undetectable for compositions higher than 0.70. In any case, we have to analyze in more detail the ($D^°-A^°$) pair transition since its evolution with the aluminum content determines the shape of the spectra.

A priori, we can associate the donor level to silicon and the acceptor one to carbon since the latter, up to now, has been found only as an acceptor in $Al_xGa_{1-x}As$.[15] An empiri-

TABLE II. Fundamental photoluminescence transition energies of $Al_xGa_{1-x}As$ ($0.38 \leqslant x \leqslant 0.84$) samples at 2 K and the E_{BE} and $E_{C_{As}}$ binding energies deduced from them.

Sample	x	Thickness (μm)	E_g^X (eV)	BE (eV)	E_{BE} (meV)	$(e^- - C_{As})$ (eV)	$E_{C_{As}}$ (meV)	$(D^\circ - A^\circ)$ (eV)
GM70	0.38	5.6	2.0746	2.0437	30.9	−	−	1.9633
GM71	0.48	4.3	2.1000	2.0631	36.9	2.0559	44.1	1.9972
GM72	0.51	3.9	2.1079	2.0682	39.7	2.0603	47.6	2.0109
GM73	0.66	2.2	2.1486	2.1012	47.4	2.0951	53.5	2.0489
GM74	0.70	1.7	2.1598	2.1117	48.1	2.1049	54.9	—
GM75	0.74	1.1	2.1713	2.1205	50.8	2.1145	56.8	—
GM76	0.79	0.8	2.1859	2.1332	52.7	2.1275	58.4	—
GM77	0.83	0.5	2.1977	2.1445	53.2	2.1387	59.0	—

as the aluminum content increases due to the fact that layers with high aluminum content are obtained from solutions with high quantities of aluminum and small fractions of arsenic. It is well known that the growth is limited by the rate at which the arsenic atoms penetrate into the interface,[32] in such a way that those layers with lower aluminum content are the thicker ones. This effect is expected if keeping in mind that all samples were grown in the same temperature range ($755-735\,°C$) and with the same cooling rate.

As an example, the result of the decomposition of two spectra are shown in Figs. 3(a) and 3(b). It can be seen in both spectra: a narrow peak of approximately 6 meV, corresponding to the BE. As we will discuss later, following the same criteria that Torres-Delgado *et al.*[18] we can infer that,

in our case, the exciton is also bound to the carbon acceptor. At the same time, at lower energies, the $(e^- - C_{As})$ transition can be found forming a shoulder, followed by the recombination of the $(D^\circ - A^\circ)$ pair at about 40–50 meV below.

The mult-Gaussian fitting procedure is a useful tool for recognizing the transitions located at energies lower than the near band gap emissions. Generally, two main peaks can be distinguished below the exciton line. The nearest and less intense one is almost equidistant from the BE transition at an energy around 32 meV in average [labeled 4 in Fig. 3(a) and labeled 5 in Fig. 3(b)]. The most intense transition and lower in energy changes its position linearly with the aluminum content [labeled 7 in Fig. 3 (b)]. Due to the constant separation from the BE, the first peak was assigned to a TO (X)-GaAs type replica; the second one fits better with a TO (X)-AlAs type rather than a LO(X)-AlAs type phonon replica. The deconvolution procedure shows the presence of small additional phonon replicas, as have been reported by others authors.[15,17,18,33,34] By comparing its energy positions and line shapes with those already reported, we also conclude that they are related to TA(X), 2TA(X) and TA(X)+LA(X) phonon replicas from both the BE and $(e^- - A^\circ)$ transitions.

The dependencies of the BE and $(e^- - A^\circ)$ transitions on x have been obtained by means of quadratic regressions. The result of the fits is shown in Fig. 4 and the relationships are
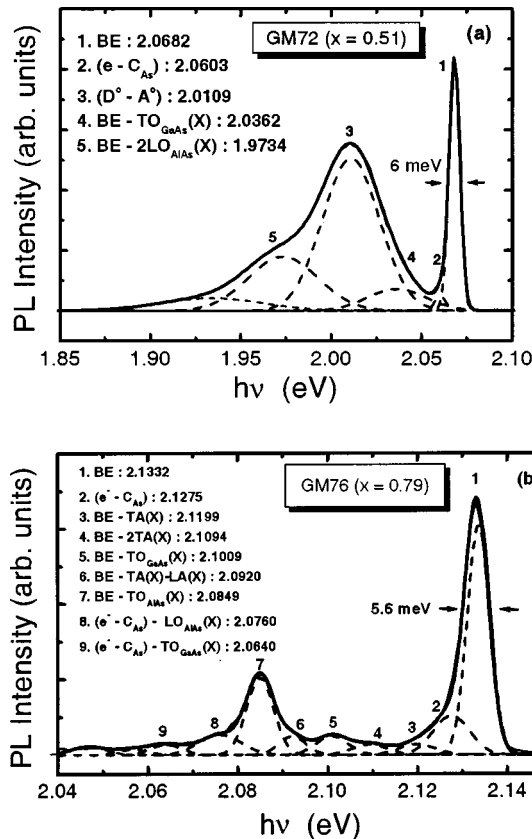

FIG. 3. Photoluminescence spectrum of the GM72 (a) and GM76 (b) samples and the mult-Gaussian fitting. The assignment of the transitions is indicated in (a) and (b).
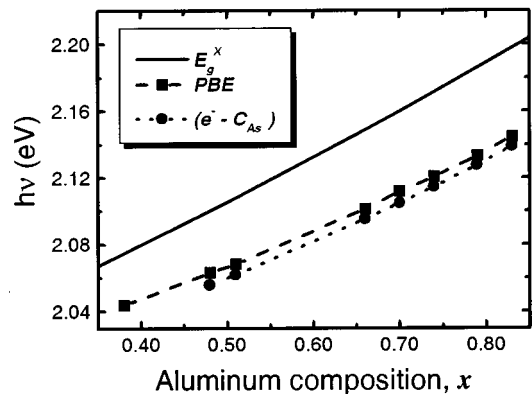

FIG. 4. Quadratic dependencies followed by the BE and $(e^- - A^\circ)$ transitions with the aluminum content in the range $0.38 \leqslant x \leqslant 0.84$. The energy gap E_g^X follows the relation: $E_g^X(x) = 1.988 + 0.207x + 0.055x^2$ (Ref. 15).
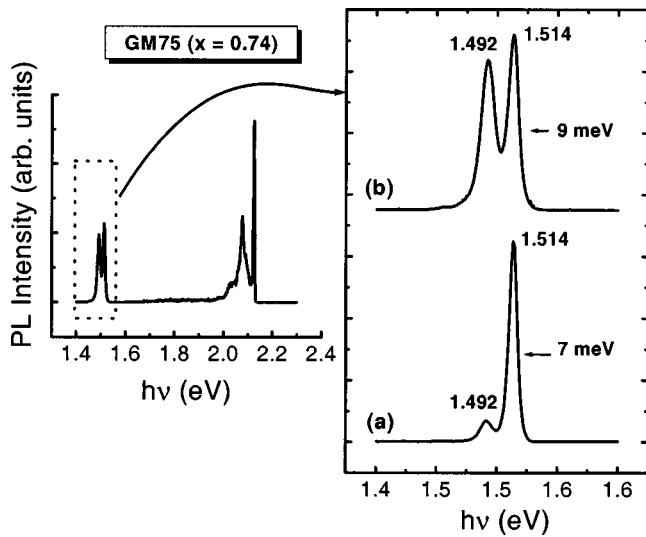
FIG. 5. Photoluminescence spectra for two samples in the characteristic energy range of the GaAs emissions. Curve (a) corresponds to a GaAs layer on (100) GaAs substrate, and (b) to a deposited $Al_{0.74}Ga_{0.26}As$ layer on the same substrate.

given by Eq. (2):

$$BE(x) = 1.9909 + 0.1010x + 0.1009x^2,$$
$$(e^- - C_{As})(x) = 1.9868 + 0.0911x + 0.1105x^2. \tag{2}$$

As can be seen from Fig. 4 and from Eq. (2), both dependencies behave in a similar way. This fact leads us to believe that the exciton that we are observing is bounded to a carbon acceptor impurity, which is one of the main residual impurities. Similar results have been reported by Torres-Delgado *et al.*[18] at 11 K for $Al_xGa_{1-x}As$ layers also grown by LPE.

Figure 5 shows two PL spectra in the characteristic energy range of the GaAs emissions. Figure 5(a) corresponds to a GaAs layer on (100) GaAs substrate, and Fig. 5(b) corresponds to sample with the same substrate but with a deposited $Al_{0.74}Ga_{0.26}As$ layer. The AlGaAs layer thickness is 1.1 μm and the 514.5 nm argon line penetrates 1.4 μm (the absorption coefficient for $x = 0.74$ is 7.28×10^3 cm^{-1}), and therefore, the photons reach the interfacial region. As can be
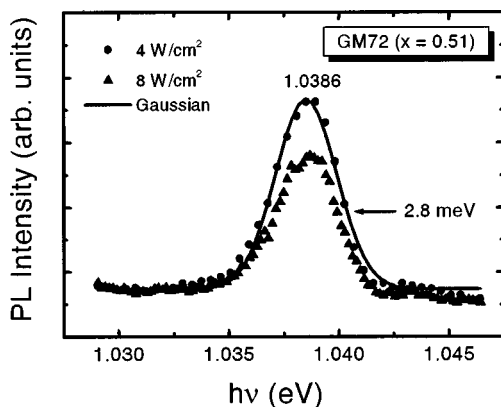

FIG. 6. New emission at 1.0386 eV found at 10 K in several of our samples under different excitation densities.
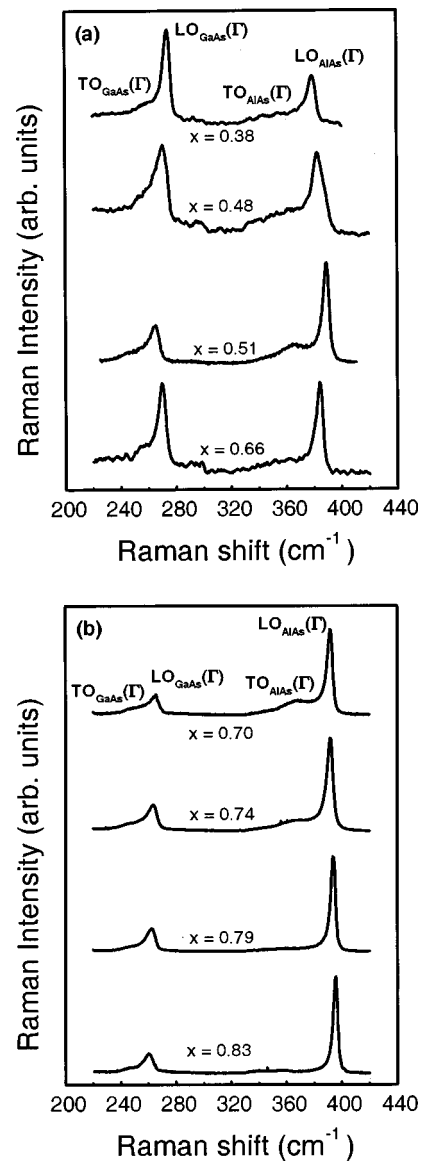

FIG. 7. Raman spectra of nonintentionally doped $Al_xGa_{1-x}As$ layers with different values of Al content ($0.38 \le x \le 0.84$).

noticed in both spectra, the excitonic emission dominates around 1.514 eV, followed by the free-electron–neutral-acceptor transition at a lower energy, 1.42 eV. Usually, the appearance and the FWHM of the BE is used as the criteria in the evaluation of the interfacial quality. It is known that local fields produced by fluctuations of the composition and location of the atoms in the crystal, as well as impurities and/or defects can cause exciton dissociation, making this transition undetectable.

The results previously obtained emphasize the conclusions of Torres-Delgado *et al.*,[10] which claim that the higher crystalline quality layers are obtained growing in near-equilibrium conditions. In addition, the broad band associated with the presence of gallium antisites and arsenic vacancies (around 1.444 eV) is not observed. This band appears when the layers are grown with certain supercooling in spite of obtaining better superficial morphology.

Finally, we have found at 10 K a very narrow emission

TABLE III. Experimental LO-phonon frequencies of $Al_xGa_{1-x}As$ samples for $0.38 \leqslant x \leqslant 0.84$.

Sample	x	Phonon frequency (cm^{-1})	
		LO_{GaAs}	LO_{AlAs}
GM70	0.38	275.07	380.28
GM71	0.48	271.44	384.34
GM72	0.51	270.86	385.14
GM73	0.66	266.06	390.43
GM74	0.70	264.66	392.09
GM75	0.74	264.30	392.97
GM76	0.79	262.81	394.76
GM77	0.83	260.57	395.94

(2.8 meV) peak at 1.0386 eV in several samples and under different excitation densities. The origin of this transition is still being investigated (Fig. 6). Deep levels related to silicon are generally found in this region.[15] It is probably a structural complex which includes silicon ($Si_{Ga}-V_{Ga}$; $Si_{Ga}-Si_{As}$), since it is known that only a fraction is incorporated as shallow donors for lower silicon concentrations; the rest is incorporated as deep donors (possibly as *DX* centers).[35–37] In a recent work on the characterization of $Al_xGa_{1-x}As$ layers grown by MOCVD, the authors reported an electron trap at a similar position: 1.03 eV. However, they relate this trap to the known EL2 level, a defect associated to an arsenic antisite.[38]

B. Raman spectroscopy

The Raman technique is a straightforward method for finding the different optical phonon energies at the Γ point, and hence, the aluminum composition of the sample. In our case, we have found a typical two-mode phonon spectra, with two sets of optical frequencies associated to the GaAs and AlAs compounds, where the intensities are proportional to the relative concentrations, as it is shown in Fig. 7.

All measurements were made in backscattering configuration. Since the samples were grown on a (100) surface, Raman selection rules allow only LO phonons to be detected in the spectra. However, at the left of each LO line, the respective transverse optical (TO) phonon can be found forming a shoulder. Since the relative intensities of the TO and LO peaks do change, we attribute the TO mode presence to crystalline disorder normal to the (001) GaAs substrate.

The experimental data are summarized in Table III. These two dependencies were fitted with a least-squares procedure that leads to the expressions:

$$\omega_{GaAs} = 366.70 + 36.95x - 1.62x^2$$

$$\omega_{AlAs} = 291.42 - 47.73x + 13.86x^2. \tag{3}$$

We have included in the fitting of our experimental results the LO phonon frequencies for $x=0$ (291.5 cm^{-1}) and $x=1$ (402.2 cm^{-1}),[15] in order to cover the complete range of aluminum composition. Figure 8 shows some of the most recent relations[21,22] and the results obtained in this work (crosses).
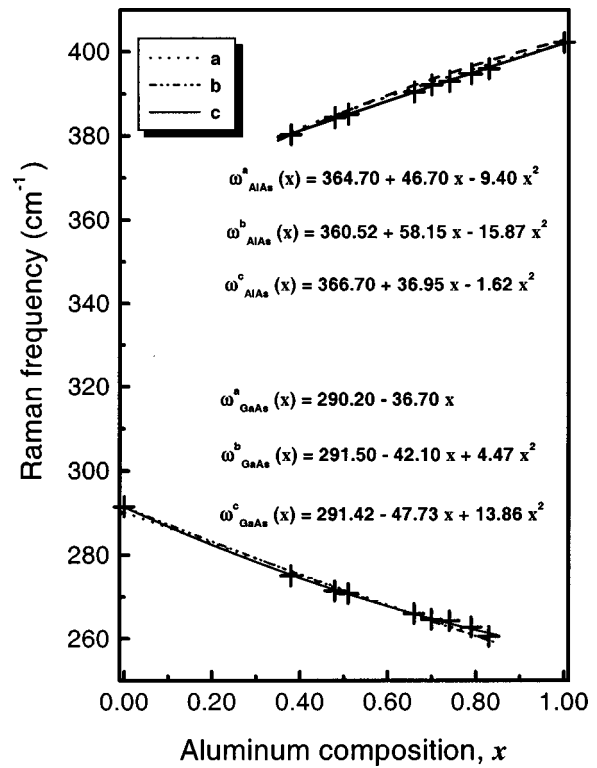

FIG. 8. The most recent quadratic relations of LO phonon frequencies as a function of AlAs mole fraction: (a) Solomon *et al.* (see Ref. 22); (b) Wasilewski *et al.* (see Ref. 21) and (c) our results.

IV. CONCLUSIONS

Photoluminescence at LT and RT Raman spectroscopy techniques were used to investigate the interfacial and crystalline quality of $Al_xGa_{1-x}As$ epitaxial layers in the $0.38 \leqslant x \leqslant 0.84$ aluminum content range. The samples have been grown by liquid phase epitaxy in near-equilibrium conditions. The close link between the intensities of the BE and $(D°-A°)$ pair transitions indicates that the exciton is bound to a carbon acceptor impurity. Furthermore, the evolution of the $(D°-A°)$ pair transition was explained from the behavior of the silicon donor binding energy as the aluminum content is increased. The quadratic compositional dependencies followed by the BE and $(e^--A°)$ emissions are reported. The presence of a narrow line (2.8 meV) around 1.0386 eV, which we believe associated to a silicon impurity, is reported. Finally, Raman measurements showed the expected quadratic variations of LO phonon frequencies with the aluminum content. These results are in good agreement with recent experiments.

[1] K. Bouamamo, W. Horig, and H. Neumann, Semicond. Sci. Technol. **13**, 75 (1998).
[2] K. Xiaoli, L. Xihua, W. Minhua, C. Dehua, and S. Nanxin, High Technol. Lett. **8**, 21 (1998).

[3] G. F. Zheng, W. Zhang, Z. Shi, D. Thorp, R. B. Bergmann, and M. A. Green, Solar Energ. Mat. Sol. Cells **51**, 95 (1998).

[4] A. Motogaito, M. Kimura, S. Dost, H. Katsuno, A. Tanaka, and T. Sukigawa, J. Cryst. Growth **182**, 275 (1997).

[5] Y. Wakagama and S. Tanaka, J. Cryst. Growth **181**, 304 (1997).

[6] R. L. Moon, J. Cryst. Growth **170**, 1 (1997).

[7] E. Kuphal, Appl. Phys. A: Solids Surf. **52**, 380 (1991).

[8] M. G. Astles, *Liquid-Phase Epitaxy of III-V Compound Semiconductors Materials and their Device Applications* (Adam Hilger, Bristol, England, 1990).

[9] L. R. Dawson, J. Cryst. Growth **27**, 86 (1974).

[10] G. Torres-Delgado, J. G. Mendoza-Álvarez, and B. E. Zendejas, Surf. Sci. **62**, 275 (1992).

[11] S. Adachi, J. Appl. Phys. **58**, R1 (1985).

[12] B. Monemar, Phys. Rev. B **8**, 5711 (1973).

[13] S. Adachi, *Properties of Aluminium Gallium Arsenide*, EMIS Data Reviews Series, Vol. 7 (INSPEC, The Institute of Electrical Engineers, London, 1993).

[14] J. S. Blakemore, J. Appl. Phys. **53**, R123 (1982).

[15] L. Pavesi and M. Guzzi, J. Appl. Phys. **75**, 4779 (1994).

[16] M. Guzzi, E. Grilli, and S. Oggioni, Phys. Rev. B **45**, 10951 (1992).

[17] H. G. M. Lochs, S. M. Olsthoorn, T. P. Huijgen, F. L. M. Spijkers, F. A. J. M. Driessen, and L. J. Giling, J. Phys.: Condens. Matter **3**, 7179 (1991).

[18] G. Torres-Delgado, R. Castanedo-Pérez, P. Díaz-Arencibia, J. G. Mendoza-Álvarez, J. L. Orozco-Vilchis, M. Murillo-Lara, and A. Serra-Jones, J. Appl. Phys. **78**, 5090 (1995).

[19] S. Logothetidis, M. Cardona, L. Tapfer, and E. Bauser, J. Appl. Phys. **66**, 2108 (1990).

[20] A. N. Pikhtin, Sov. Phys. Semicond. **11**, 245 (1977).

[21] Z. R. Wasilewski, M. M. Dion, D. J. Lockwood, and P. Poole, J. Appl. Phys. **81**, 1683 (1997).

[22] G. S. Solomon, D. Kirillov, H. C. Chui, and J. S. Harris, J. Vac. Sci. Technol. B **12**, 1078 (1994).

[23] G. Torres-Delgado, P. Díaz-Arencibia, J. G. Mendoza-Álvarez, R. Castanedo, J. L. Orozco-Vilchis, M. Murillo-Lara, and A. Serra-Jones, AIP Conf. Proc. **378**, 239 (1996).

[24] U. S. Qurashi, M. Zafar Iqbal, and T. G. Andersson, J. Appl. Phys. **80**, 5932 (1996).

[25] M. B. Panish and M. Ilegems, *Progress in Solid State Chemistry* (Pergamon, New York, 1969).

[26] C. Bocchi, C. Ferrari, and P. Franzosi, Nuovo Cimento D **13**, 1 (1991).

[27] G. Kühn, A. Zehe, D. Sutter, P. Streubel, and H. Neels, Krist. Tech. **10**, 963 (1975).

[28] M. Ilegems and G.L. Pearson, *Proceedings of 2nd International Symposium on GaAs* (Institute of Physics, Bristol, 1968), p. 3.

[29] R. Heilmann and G. Olegart, Semicond. Sci. Technol. **5**, 1040 (1990).

[30] N. Chand, T. Henderson, J. Klem, W. T. Masselink, R. Fischer, Y. Chang, and H. Morkoc, Phys. Rev. B **30**, 4481 (1984).

[31] J. C. M. Henning, J. P. M. Ansems, and P. J. Roksnoer, Semicond. Sci. Technol. **3**, 361 (1988).

[32] M. C. Wu and Y. K. Su, J. Cryst. Growth **96**, 52 (1989).

[33] T. F. Kuech, P. J. Wolford, K. R. Potems, J. A. Bradley, K. H. Kelleher, D. Yang, J. P. Forrell, P. M. S. Lesser, and F. H. Pollak, Appl. Phys. Lett. **51**, 505 (1987).

[34] G. Olegart, R. Mitdank, and P. Heidborn, Semicond. Sci. Technol. **8**, 1966 (1993).

[35] P. L. Souza and E. V. K. Rao, J. Appl. Phys. **67**, 7013 (1990).

[36] N. Galbiati, E. Grilli, M. Guzzi, L. Brusaferri, L. Pavesi, and H. Henini, in *Proceedings of 23rd International Conference on The Physics of Semiconductors*, edited by M. Scheffler and R. Zimmermann (World Scientific, Singapore, 1996), Vol. 2, p. 1575.

[37] E. P. Visser, X. Tang, R. W. Wieleman, and L. J. Gilling, J. Appl. Phys. **69**, 3266 (1991).

[38] J. Darmo, F. Dubecky, H. Hardtdegen, M. Hollfelder, and R. Schmidt, J. Cryst. Growth **186**, 13 (1998).